

Chapter 15

Spatial Distribution and Radiological Risk Quantification of Natural Radioisotopes in the St. Martin's Island, Bangladesh



Rahat Khan, Md. Abu Haydar, Sudipta Saha, Md. Masud Karim, Md. Ahsan Habib, Md. Bazlar Rashid, Abubakr M. Idris, and Debasish Paul

Abstract The radioactivity concentrations of ^{226}Ra , ^{232}Th and ^{40}K were measured by HPGe gamma-ray spectroscopy in beach sand and water samples collected from and around the only coral reefed Island (St. Martin's), in the Bay of Bengal. Average activity concentrations of ^{226}Ra , ^{232}Th and ^{40}K are 15.53, 15.42 and 372.32 Bq kg $^{-1}$ for beach sand samples, and 4.96, 4.67 and 22.78 Bq kg $^{-1}$ for water samples, respectively. No artificial radionuclides (e.g., ^{134}Cs , ^{137}Cs) were detected in any of the analyzed samples. Lower activity concentrations of sand samples compared to those of other coastal areas of the Bay of Bengal may be due to the thick coral reef of this island. The estimated radiation hazard parameters including radium equivalent activity, radiation hazard index, annual effective dose rate, absorbed dose rate and excess lifetime cancer risk are lower than the permissible limits. In terms of radiological parameters, this island is quite safe for tourism.

Keywords Coral reefed island · Naturally occurring radionuclides · Beach sand and water · Radiological hazard indices · St. Martin's Island · Bangladesh

R. Khan (✉) · Md. A. Haydar · S. Saha · Md. M. Karim · D. Paul
Institute of Nuclear Science & Technology, Bangladesh Atomic Energy Commission, Savar,
Dhaka 1349, Bangladesh
e-mail: rahatkhan.baec@gmail.com

Md. A. Habib · Md. B. Rashid
Geological Survey of Bangladesh, Segunbaghicha, Dhaka 1000, Bangladesh

A. M. Idris
Department of Chemistry, College of Science, King Khalid University, Abha 62529, Saudi Arabia
e-mail: abubakridris@hotmail.com

Research Center for Advanced Materials Science (RCAMS), King Khalid University, Abha 62529, Saudi Arabia

15.1 Introduction

Beach sands are mostly composed of those minerals which are resistant to wave abrasion, (e.g., quartz, feldspar). A combination of weathering, degradation and fragmentation processes supply those wave resistant minerals to the coastal areas (Papadopoulos et al. 2016 and the reference therein). A number of coastal areas in and around the Bay of Bengal have already been reported for higher level of natural radioisotopes (e.g., ^{226}Ra , ^{232}Th and ^{40}K) owing to the presence of wave resistant placer minerals such as ilmenite, zircon, monazite, garnet, rutile etc. (Khan et al. 2019a, 2021; Rao et al. 2009; Mohanty et al. 2004; Kannan et al. 2002; Alam et al. 1999). These naturally occurring radionuclides (NORMs) could cause numerous radiological health risks including different types of cancers, kidney malfunction, bone deformities etc. (e.g., Habib et al. 2022; Khan et al. 2019b and the references therein) owing to the ionizing radiation emission and radon inhalation. Thus considering the highest contribution of external dose to the human by the natural radiation, the assessments of radiological distribution along with their associated potential health risks are of huge importance (Habib and Khan 2021; UNSCEAR 2000).

Unlike the other islands of the Bay of Bengal, St. Martin's Island (Bangladesh) is one of the few islands in the world which is surrounded by thick coral reefs. St. Martin's Island is of great ecological importance as it is the only fossiliferous marine island in the Bay of Bengal which possesses huge areas of sandy beach and mangrove formations (Tomascik 1997). This is one of the most beautiful domestic and foreign tourist destinations in Bangladesh since it possesses attractive natural sceneries, clear sea-site, and natural beauties of coral colonies. Coral reefs as 'rainforests of the sea' engage only <0.1% of the world's total marine area, but they supply accommodations, breeding environments and food to the more than 25% of all aquatic botanical and zoological species (Islam et al. 2019 and the reference therein). Considering the marine ecological significance, millions of peoples dependence (as tourists and/or inhabitants) and scientific importance of coral reefs, several studies on heavy metal accumulations in corals, marine sediments and sea water along with their associated health and ecological risk assessment have been performed (Joy et al. 2019; Jafarabadi et al. 2017a, 2018a, b; Prouty et al. 2013; Mokhtar et al. 2012). Along with the heavy metal distribution, *n*-alkanes, polycyclic aromatic hydrocarbons and persistent organic pollutants distribution in coral-associated environmental compartments have also been reported by Jafarabadi et al. (2017b, 2018c, d). Furthermore, geochemistry and precise elemental ratios in coral skeletons and associated environmental compartments have long been used to explain the climate change, to reconstruct the temporal pollution history and to assess the sea water quality (Saha et al. 2016, 2018, 2019; Lewis et al. 2018; Prouty et al. 2010). However, the studies on NORMs distribution in the coral reefed Island and their associated radiological health risks (Lin et al. 2019) coral reefs in the South China Sea) are very much scarce. Islam et al. (2019) reported radioactivity concentrations of coral skeleton and the marine sediments around the St. Martin's Island, leaving the beach sand (or, soil) and the seawater in and around the Island. Thus, geological variation and variability

of environmental compartments (e.g., marine sediments, coral skeletons, seawater, beach sands or soils) invoke similar radiological studies in various environmental compartments in and around the coral reefs of the world to provide a comprehensive scenario to the scientific community as well as to the tourists and local inhabitants.

Study of radiological health hazards owing to the NORMs is very much important for the safety of the tourists as well as the local inhabitants. It is also essential to measure the baseline level of NORMs in different environmental sections (e.g., beach sand, water, marine sediment and coral backbone) before any pollution events (e.g., nuclear weapon test, nuclear reactor accidents etc.) commence nearby. However, a comprehensive study on the distribution of NORMs in the beach-sand and water samples across and around this island has not hitherto been done. Thus, the present study aims at the determination of NORMs (^{226}Ra , ^{232}Th and ^{40}K) as well as search for the anthropogenic radionuclides (e.g., ^{134}Cs , ^{137}Cs) in beach sand and water samples taken from the St. Martin's Island's surroundings to evaluate the baseline distribution of radionuclides and to estimate the potential radiological risks.

15.2 Materials and Methods

15.2.1 Area of Interest

St. Martin's Island (area: $\sim 8 \text{ km}^2$) resides in the north-eastern side of the Bay of Bengal and southernmost part of Bangladesh which is about 9 km south of the Cox's Bazar-Teknaf peninsula (Fig. 15.1). Length of this Island (south-north side) is approximately 5.6 km and the width (east-west side) varies from 200 to 700 m. The island is almost flat and is about 3.6 m above the average sea level (Akhtar 1992). St. Martin's Island represents the westernmost extent of the Arakan Yoma uplift and it is ringed by a boulder field in the intertidal zone along the southern and western shore of the Island (Khan 1964).

15.2.2 Sampling and Sample Processing

Samples (sand and water) were collected along the coast line of St. Martin's Island by January 2017. Beach sand samples were taken from 15 different sampling stations (separated each other by $\geq 500 \text{ m}$) covering both the east and west side of the sandy beaches as shown in Fig. 15.1. From each sampling points, approximately 1.5 kg of superficial sand samples were taken (sampling depth: $\sim 10 \text{ cm}$). Collected samples were then instantly preserved in airtight clean and properly marked zip-lock polyethylene bags and moved to the sample preparation laboratory for subsequent analysis. After eliminating the extraneous matters including stones, gravels, pebbles, roots and botanical debris, the samples were homogeneously powdered, weight and dried

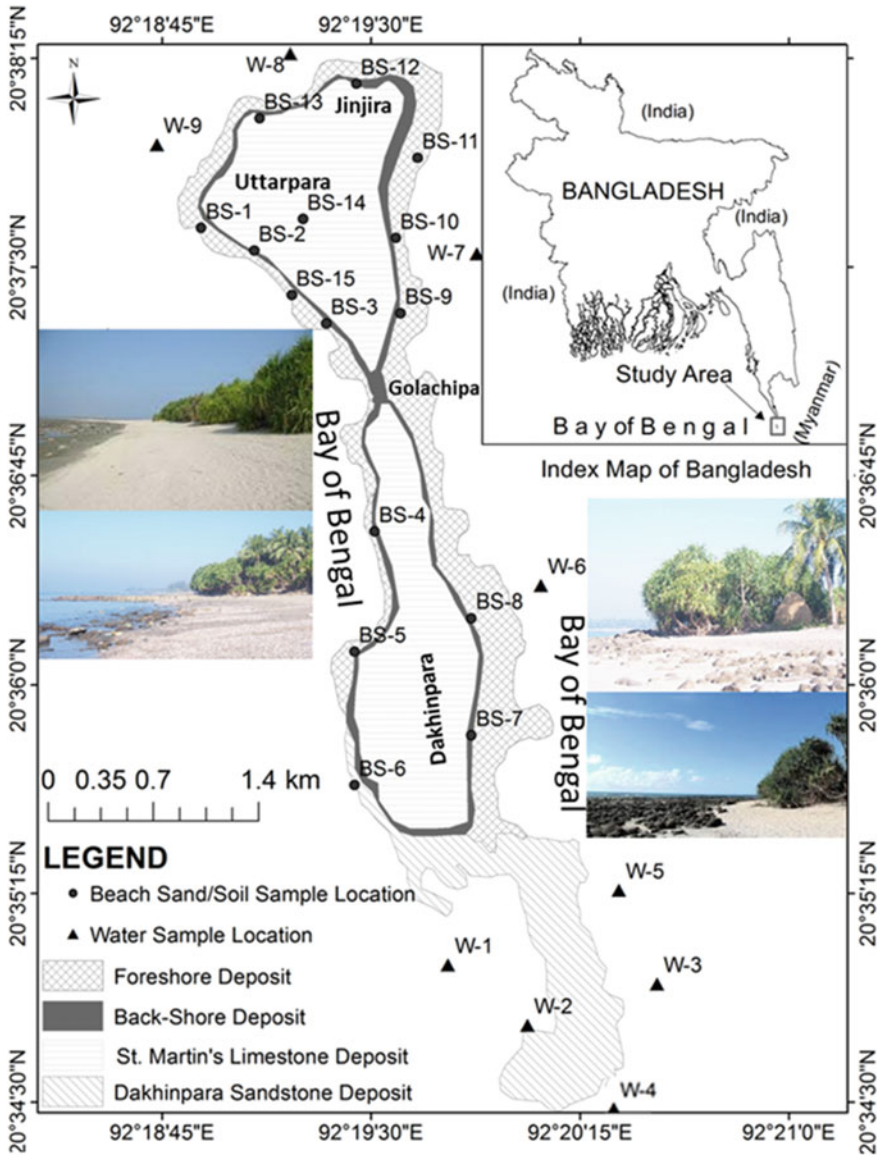


Fig. 15.1 Map shows the sampling points at St. Martin's Island, Bangladesh

(at 105 °C) until attaining the constant weight. Thereafter homogenous dried powder samples (~250 g) were hermetically packed in a cylindrical plastic pot (dimensions of the pot are identical to that of Khan et al. 2019b) and then sealed hermetically to avoid the loss of NORMs (as radon) and subsequently stored for at least 28 days at room temperature to attain the secular equilibrium among ²³⁸U and ²³²Th decay

series along with the respective daughter products (Habib et al. 2018, 2019) prior to being measured. The details of the sampling preparation procedures were previously reported elsewhere (Begum et al. 2022; Habib et al. 2018, 2019; Khan et al. 2022, 2019b).

Sea surface water samples were collected from 9 different spots (Fig. 15.1) around the Island. From each spot, about 1.5 L of water was taken in clean, acid (diluted HNO₃) rinsed and dried plastic container. The collected water samples in the plastic container were immediately acidified (pH ~ 1) with nitric acid to prevent adsorption of NORMs onto the walls of containers (Agbalagba and Onoja 2011) and transferred to the sample processing laboratory. The collected samples were then poured into cylindrical plastic containers of equal size and shape (of volume 260 ml). Sealing and storing of the water sample containers prior to the gamma-ray counting are same as those of sand samples.

15.2.3 Analytical Procedure

15.2.3.1 Radioactivity Measurement by Gamma Spectrometry

Analytical procedures of measuring the NORMs (²²⁶Ra, ²³²Th and ⁴⁰K) and searching the potential artificial radionuclides (¹³⁴Cs and ¹³⁷Cs) were identical to those of our previous studies (Khan et al. 2019b; Majlis et al. 2022; Habib et al. 2018, 2019). Briefly, coaxial p-type high purity Ge gamma detector with 40% relative efficiency was used in this study. In direct measurement of ²²⁶Ra and ²³²Th (measuring from the activities of their progenies) and direct measurement of ⁴⁰K were performed by following Khan et al. (2019b). Other than the naturally occurring radionuclides (²²⁶Ra, ²³²Th and ⁴⁰K), artificial radionuclides such as ¹³⁴Cs (604.5 and 795.8 keV) and ¹³⁷Cs (661.6 keV) were also searched in each analyzed samples. Blank correction, energy and efficiency calibration were similar to that of Khan et al. (2019b).

Radioactivity concentrations of NORMs in the beach sand and the seawater samples were measured from the net count rate, counting efficiency and emission probability of specific radionuclides and mass (for beach sand) or volume (for water sample) of the sample by the Eqs. (15.1) and (15.2):

$$A \text{ (Bq)} = \frac{\text{cps}_{\text{sample}} - \text{cps}_{\text{BG}}}{\varepsilon(E) \times P_{\gamma}} \quad (15.1)$$

$$\text{AC (Bq kg}^{-1}\text{)} = \frac{A}{m} \quad (15.2)$$

where, A is the radioactivity (in Bq); AC, radioactivity concentration (in Bq kg⁻¹); cps_{sample}, counts per second for the sample (in s⁻¹); cps_{BG}, Counts per second for the background (in s⁻¹); ε(E_γ), counting efficiency of the HPGe gamma-ray detector; P_γ, the emission probability; m, sample mass (kg). In this study, the minimum detectable

activity (MDA) for the gamma-ray measuring system was computed by the Eq. (15.3) (Asaduzzaman et al. 2015; Khandaker et al. 2012, 2016, 2017):

$$\text{MDA}(\text{Bq kg}^{-1}) = \frac{C_F \times \sqrt{B}}{\varepsilon(E_\gamma) \times P_\gamma \times t \times m} \quad (15.3)$$

where, C_F is the statistical coverage factor (=1.64) for 95% confidence level; B is the background counts over the region of interest for each radionuclide; $\varepsilon(E_\gamma)$, the absolute efficiency of the HPGe detector; P_γ , the emission probability; t , the measuring time in seconds and m , the mass of the sample (in kg).

15.2.4 Data Presenting Processes

Basic descriptive analysis was done for measured NORMs (variables) in our sample suits. Pearson's correlation analysis was performed to define the degree of association and interdependency existing among the determined and estimated variables parameters both radionuclides and corresponding radiological hazard indices using SPSS (version 20) software. The Inverse Distance Weighting (IDW) method was applied to interpolate the measured parameters at unmeasured locations from the observations of its values at nearby points by using ArcGIS 10.3 software. It is commonly used for displaying the spatial distribution of interested parameters in the determined beach sand samples of the mapped area (Habib et al. 2018).

15.3 Results and Discussion

15.3.1 Distribution of Radionuclides

In beach sand samples, the radioactivity level (Table 15.1) of ^{226}Ra , ^{232}Th and ^{40}K were found to be 8.79 ± 2.45 to $29.12 \pm 2.66 \text{ Bq kg}^{-1}$, 8.68 ± 3.41 to $24.72 \pm 8.70 \text{ Bq kg}^{-1}$ and 166.17 ± 68.01 to $472.53 \pm 74.44 \text{ Bq kg}^{-1}$, respectively. The obtained average values for these nuclides (Table 15.2) along with their standard deviations were 15.53 ± 5.09 , 15.42 ± 5.61 and $372.32 \pm 78.87 \text{ Bq kg}^{-1}$, respectively. The activities of ^{226}Ra , ^{232}Th and ^{40}K across the sampling points did not vary widely (Fig. 15.2, Table 15.2). Spatial distributions of ^{226}Ra , ^{232}Th and ^{40}K in our studied area are showed by inverse distance weighting (IDW) map (Fig. 15.3). Figure 15.3a, b, c and d represent the spatial distribution patterns of activity contents of ^{226}Ra , ^{232}Th , ^{40}K and absorbed dose rate, respectively in the mapped area. In the Island, radioactivity distribution maps show almost uniform partitioning. Touristic areas (northern part of the Island: Jinjira and Uttarpara) possess relatively lower activity of ^{226}Ra (Fig. 15.3a). This work pointed some trivial hot spots in some sites (eastern side

Table 15.1 Radioactivity concentrations in beach sand (BS) and soil (SL) samples collected from St. Martin Island, Bangladesh along with their associated radium equivalent activity (R_{eq} in Bq kg^{-1}), external hazard index (H_{ex}), absorbed dose rate (D in $\eta\text{Gy h}^{-1}$), annual effective dose rate (E_{ff} in $\eta\text{Gy h}^{-1}$) and excess lifetime cancer risk (ELCR)

Sample ID	Activity concentrations (Bq kg^{-1})						Radiological indices				
	^{226}Ra	\pm	^{232}Th	\pm	^{40}K	\pm	R_{eq}	H_{ex}	D	E_{ff}	ELCR
BS-1	9.45	2.37	16.27	4.39	264.38	67.20	53.07	0.143	25.44	0.031	1.10×10^{-4}
BS-2	14.17	2.47	15.18	1.40	361.87	70.86	63.74	0.172	30.97	0.038	1.33×10^{-4}
BS-3	14.18	2.29	12.11	1.40	293.59	64.91	54.10	0.146	26.24	0.032	1.13×10^{-4}
BS-4	13.81	2.35	8.68	3.41	416.90	69.76	58.32	0.158	29.03	0.036	1.25×10^{-4}
BS-5	16.66	2.42	14.23	1.48	389.11	68.41	66.97	0.181	32.65	0.040	1.41×10^{-4}
BS-6	12.52	2.59	10.67	1.42	472.53	74.44	64.16	0.173	31.98	0.039	1.38×10^{-4}
BS-7	16.27	2.45	24.69	4.58	437.28	69.81	85.25	0.230	40.99	0.050	1.76×10^{-4}
BS-8	29.12	2.66	20.42	1.61	355.70	71.14	85.71	0.231	40.87	0.050	1.76×10^{-4}
BS-9	18.25	2.55	10.99	1.37	409.07	71.92	65.46	0.177	32.20	0.040	1.39×10^{-4}
BS-10	13.86	2.48	12.61	1.49	355.77	69.66	59.29	0.160	28.97	0.036	1.25×10^{-4}
BS-11	8.79	2.43	24.72	8.70	406.81	71.53	75.46	0.204	36.29	0.045	1.56×10^{-4}
BS-12	18.48	2.49	24.63	4.93	398.48	70.06	84.38	0.228	40.36	0.050	1.74×10^{-4}
BS-13	14.8	2.39	14.8	1.48	429.92	68.64	69.07	0.187	33.84	0.042	1.46×10^{-4}
BS-14	21.62	3.15	12.01	1.85	427.25	88.72	71.69	0.194	35.14	0.043	1.51×10^{-4}
BS-15	10.93	2.38	9.30	1.31	166.17	68.01	37.02	0.100	17.71	0.022	0.76×10^{-4}

Associated uncertainties are due to the counting statistics

of Dakhinpara) of the island showing relatively higher activity of measured radionuclides, except for ^{40}K (which distributed mainly in the western side of Dakhinpara). However, trivial hot spots and consequential minute inhomogeneous distribution of NORMs do not essentially invoke any radiological risk.

The descriptive statistics of the measured values of our study are compared to those of previously published works (Rudnick and Gao 2014; Huang et al. 2015; Ghosal et al. 2017; Alam et al. 1999; Kannan et al. 2002; Khandaker et al.

Table 15.2 Comparison of radioactivity concentrations and associated radiological hazard indices of this study to those of literature data

Sample ID	Activity concentrations (Bq kg ⁻¹)			Radiological indices				
	²²⁶ Ra	²³² Th	⁴⁰ K	R _{eq}	H _{ex}	D	E _{if}	ELCR
<u>This study</u>								
Mean (n = 15)	15.53	15.42	372.32	66.25	0.179	32.18	0.040	1.39 × 10 ⁻⁴
SD (1σ)	5.09	5.61	78.87	13.33	0.036	6.33	0.008	0.27 × 10 ⁻⁴
RSD (%)	32.8	36.4	21.2	20.1	20.1	19.7	19.7	19.7
Median	14.18	14.23	398.48	65.46	0.177	32.20	0.040	1.39 × 10 ⁻⁴
Min.	8.79	8.68	166.17	37.02	0.100	17.71	0.022	0.76 × 10 ⁻⁴
Max.	29.12	24.72	472.53	85.71	0.231	40.99	0.050	1.76 × 10 ⁻⁴
<u>Literature data</u>								
World avg. ^a	35	30	400	370	1	55	0.06	2.90 × 10 ⁻⁴
UCC ^b	33	43	720	149.93	0.40	72.0	0.09	3.09 × 10 ⁻⁴
Xiamen Island, China ^c	14.6 (7.9 – 25.7)	10.9 (6.7 – 41.4)	396.4 (197.4 – 487.6)	60.71	0.164	29.9	0.04	1.29 × 10 ⁻⁴
Coastal Odisha, India ^d	273.93 (24.6 – 532.7)	2489.23 (394.5 – 4520.8)	683.23 (26.6 – 1295.4)	3886.14	10.493	1705.4	2.10	73.4 × 10 ⁻⁴
Beach soil, Cox's Bazar, Bangladesh ^e	18.9 (10.8 – 27.3)	36.7 (27.4 – 49.4)	458.2 (117 – 688)	106.66	0.288	50.5	0.06	2.18 × 10 ⁻⁴
Black sand, Langkawi Island, Malaysia ^f	1478.2 (451 – 2411)	718.2 (232 – 1272)	102.8 (61 – 136)	2513.14	6.789	11133.1	1.39	48.8 × 10 ⁻⁴
White sand, Langkawi Island, Malaysia ^f	9.78 (8.3 – 13.7)	5.87 (4.5 – 9.4)	102 (85 – 133)	26.03	0.070	12.4	0.02	0.53 × 10 ⁻⁴
Giresun sea beach, Turkey ^g	21 (2 – 44)	14 (2 – 27)	531 (23 – 1306)	81.91	0.221	40.4	0.05	1.74 × 10 ⁻⁴
Penang Island, Malaysia ^h	23 (8 – 43)	19 (9 – 43)	243 (68 – 478)	68.88	0.186	32.5	0.04	1.40 × 10 ⁻⁴

(continued)

Table 15.2 (continued)

Sample ID	Activity concentrations (Bq kg ⁻¹)			Radiological indices					
	²²⁶ Ra	²³² Th	⁴⁰ K	R _{eq}	H _{ex}	D	E _{ff}	ELCR	
Miami Bay, Penang, Malaysia ^a	1023 (24 – 2641)	2086 (37 – 5622)	381 (296 – 495)	4035.32	10.898	1787.0	2.20	7.69 × 10 ⁻⁴	
Preta beach, Brazil ⁱ	121 (54 – 180)	239 (128 – 349)	110 (47 – 283)	471.24	1.273	209.2	0.26	9.01 × 10 ⁻⁴	
Dois Rios beach, Brazil ⁱ	40 (6 – 78)	48 (12 – 87)	412 (269 – 527)	140.36	0.379	65.4	0.08	2.82 × 10 ⁻⁴	
Kalpakkam beach, India ^a	16 (5 – 71)	119 (15 – 776)	406 (200 – 854)	217.43	0.587	98.3	0.12	4.23 × 10 ⁻⁴	
West coast, Sri Lanka ^k	299 (BDL – 1243)	1032 (14 – 6257)	335 (BDL – 647)	1800.56	4.862	794.6	0.98	34.2 × 10 ⁻⁴	
Black sea shore, Romania ^l	6.7 (2.9 – 14)	3.7 (1.2 – 8.5)	69 (9 – 282)	17.30	0.047	8.3	0.01	0.36 × 10 ⁻⁴	
Marine sediment, St. Martin's Island ^m	30.7 (24.5 – 39.5)	36.8 (28.3 – 47.4)	388 (358 – 422)	113.20	0.306	53.1	0.07	2.29 × 10 ⁻⁴	
Coral skeletons, St. Martin's Island ^m	16.5 (11.7 – 21.9)	28.7 (23.3 – 32.8)	334 (322 – 346)	83.26	0.225	39.3	0.05	1.69 × 10 ⁻⁴	

^a UNSCEAR (2000)

^b Upper Continental Crust (UCC-calculated data); Rudnick and Gao (2014)

^c Huang et al. (2015)

^d Ghosal et al. (2017), Alam et al. (1999)

^f Khandaker et al. (2018)

^g Kucukomeroglu et al. (2016)

^h Shuaibu et al. (2017)

ⁱ Freitas and Alencar (2004)

^j Kannan et al. (2002)

^k Mahawatte and Fernando (2013)

^l Margineanu et al. (2013)

^m Islam et al. (2019)

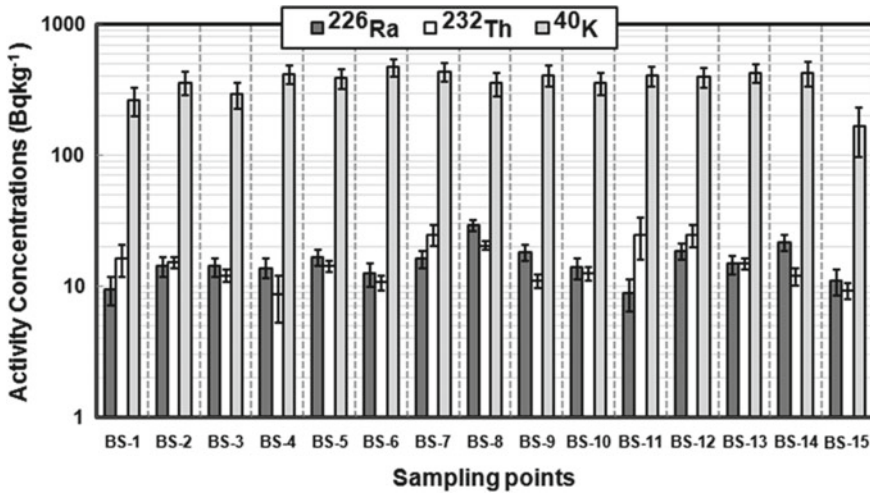


Fig. 15.2 Variation of activity concentrations of beach sand and soil samples of St. Martin's Island, Bangladesh at different sampling locations

2018; Kucukomeroglu et al. 2016; Shuaibu et al. 2017; Freitas and Alencar 2004; Mahawatte and Fernando 2013; Margineanu et al. 2013; Islam et al. 2019) in Table 15.2. The radionuclides concentrations of St. Martin's Island of this work are significantly lower than the other coastal areas known for higher background radiation (e.g., Khandaker et al. 2018; Shuaibu et al. 2017; Freitas and Alencar 2004). Specific activities of ^{226}Ra and ^{40}K of this study are comparable to those of beach sand of Cox's Bazar, Bangladesh (Alam et al. 1999) whereas activity concentration of ^{232}Th shows opposite trend which implies that Th-rich monazite is less abundant in St. Martin's Island compared to the mainland (Cox's Bazar) of Bangladesh. Disregarding the variation of activity concentrations, Kalpakkam beach, India (Kannan et al. 2002) shows similar trend as those of Cox's Bazar beach, Bangladesh with our study. However, the activity concentrations in our study are significantly lower than the other coastal areas of the Bay of Bengal, including Coastal Odisha, India (Ghosal et al. 2017) and West coast, Sri Lanka (Mahawatte and Fernando 2013). A reasonable assumption for such lower activity concentrations of our study compared to those of other coastal areas of the Bay of Bengal (Alam et al. 1999; Kannan et al. 2002; Ghosal et al. 2017; Khan et al. 2017, 2018) can be explained in terms of coral abundances and the ocean current dynamics around the St. Martin's Island. Activity concentrations of ^{226}Ra and ^{232}Th in the beach sands of the present study are significantly lower (Table 15.2) than the marine sediments (Islam et al. 2019) around the St. Martin's Island, while the activity concentration of ^{40}K are almost comparable among them. ^{232}Th -radioactivity is ~ 1.8 times lower in the beach sand than that of coral skeleton, whereas the specific activities of ^{226}Ra and ^{40}K in beach sand are comparable to those of coral skeleton. The comparable radioactivity concentration of ^{40}K in beach sands, marine sediments and coral skeleton may be explained in

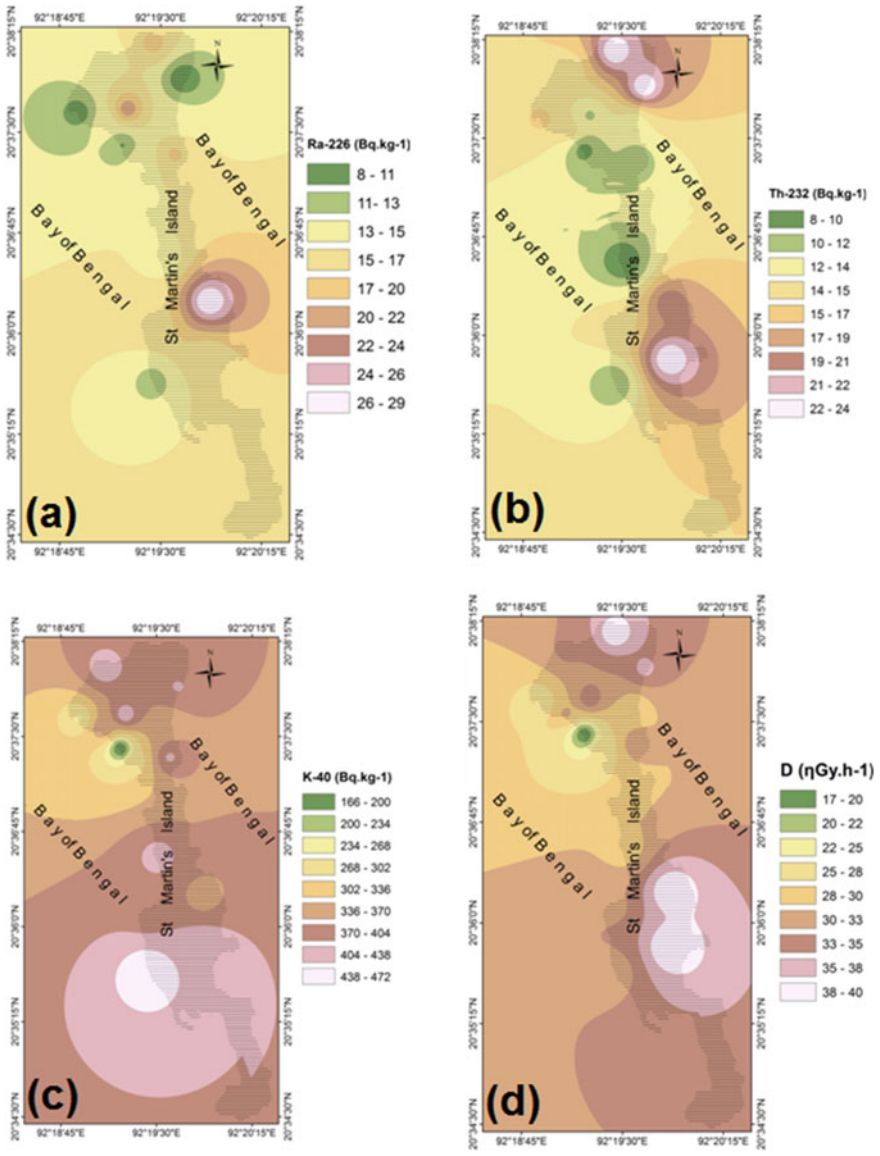


Fig. 15.3 Inverse distance weighting (IDW) map for the spatial distribution of activity concentrations of **a** ^{226}Ra , **b** ^{232}Th , **c** ^{40}K and **d** estimated dose distribution in the St. Martin's Island, Bangladesh

terms of K-solubility and the distribution of terrigenous minerals like K-feldspar (KAlSi_3O_8) and mica ($\text{KAlSi}_4\text{O}_{10}$).

Along with the beach sand samples, the radioactivity concentrations of sea surface water samples were also measured for the 9 marine spots around the St. Martin's Islands. Specific activity level of ^{226}Ra , ^{232}Th and ^{40}K in water samples with their associated descriptive statistics and some relevant literature data (Zare et al. 2015; Baltas et al. 2017; Almayahi et al. 2012) are presented in Table 15.3. In sea-water

Table 15.3 Radioactivity concentrations of water samples collected around the St. Martin Island are compared to those of sea water in previous works

Sample ID	Activity concentration (Bq kg^{-1})					
	^{226}Ra	\pm	^{232}Th	\pm	^{40}K	\pm
<i>This study</i>						
W-1	7.78	0.29	3.89	0.06	BDL	
W-2	1.32	0.28	5.68	0.14	41.00	1.59
W-3	BDL		0.68	0.07	BDL	
W-4	1.36	0.22	4.23	0.13	BDL	
W-5	BDL		5.48	0.15	BDL	
W-6	6.39	0.22	4.64	0.16	BDL	
W-7	9.54	0.30	10.41	0.17	BDL	
W-8	0.56	0.22	4.41	0.12	BDL	
W-9	7.78	0.29	2.59	0.10	BDL	
Mean	4.96		4.67			
SD (1σ)	3.75		2.64			
RSD (%)	75.6		56.5			
Median	6.39		4.41			
Min.	BDL		0.68		BDL	
Max.	9.54		10.41		41.00	
<i>Literature data</i>						
Oman Sea ^a	2.50 (2.19 – 2.82)		1.90 (1.66 – 2.17)		141.48 (132.60 – 148.87)	
Black Sea in Rize, Turkey ^b	0.26 (0.16 – 0.63)		0.11 (0.07 – 0.17)		5.42 (3.44 – 6.20)	
Northern Peninsula, Malaysia ^c	3.46 (2.33 – 7.03)		3.63 (1.58 – 8.64)		190.2 (150 – 220)	

BDL: Bellow detection limit

^a Zare et al. (2015)

^b Baltas et al. (2017)

^c Almayahi et al. (2012)

samples the specific activities of ^{226}Ra , ^{232}Th and ^{40}K were found to be below detection limit (BDL) to $9.54 \pm 0.30 \text{ Bq kg}^{-1}$, 0.68 ± 0.07 to $10.41 \pm 0.17 \text{ Bq kg}^{-1}$ and BDL to $41.00 \pm 1.59 \text{ Bq kg}^{-1}$, respectively. None of the analyzed samples (both sand and water) contains detectable amount of artificial radionuclides (here, ^{134}Cs and ^{137}Cs). The average values of minimum detectable activities (MDAs) of ^{226}Ra , ^{232}Th , ^{40}K , ^{134}Cs and ^{137}Cs in the determined sand samples are 0.48, 0.35, 18.8, 0.50 and 0.41 Bq kg^{-1} , respectively whereas for water samples MDAs for those radionuclides are 0.52, 0.38, 20.2, 0.53 and 0.45 Bq L^{-1} , respectively.

15.3.2 Radiological Risk Assessment

To assess the potential radiological risks owing to the natural radioisotope in beach sand of this highly touristic area (St. Martin's Island, Bangladesh), radium equivalent activity (Ra_{eq}), radiation hazard index (H_{ex}), absorbed dose rate (D), annual effective dose rate (E_{ff}) and excess lifetime cancer risk (ELCR) were calculated in the current research.

15.3.2.1 Radium Equivalent Activity (Ra_{eq})

To assess the combined radiological threat to the population, Ra_{eq} has widely been used which is attained from the activity concentrations of ^{226}Ra , ^{232}Th and ^{40}K (Khan et al. 2019b and the references therein). Most of the radiation dose received by human being is due to the emission of gamma radiation from natural radiation sources (Tufail 2012), including ^{40}K and the progeny of the ^{238}U and ^{232}Th decay series. Owing to the potential disequilibrium among ^{226}Ra and its progenies, radionuclides (^{226}Ra , ^{232}Th) may not be evenly distributed in the environmental geochemical samples (e.g., sediment, soil, sand, etc.) (Ahmed et al. 2014). Thus, for homogeneous exposure calculation, the radioactivity concentrations are expressed as Ra_{eq} (in Bq kg^{-1}) which can be calculated by the following expression:

$$Ra_{eq}(\text{Bq kg}^{-1}) = A_{226\text{Ra}} + 1.43A_{232\text{Th}} + 0.077A_{40\text{K}} \leq 370 \quad (15.4)$$

where, $A_{226\text{Ra}}$, $A_{232\text{Th}}$ and $A_{40\text{K}}$ are activity concentrations of ^{226}Ra , ^{232}Th and ^{40}K (in Bq kg^{-1}), respectively. In our studied area Ra_{eq} ranges from 37.02 to 85.71 Bq kg^{-1} (Table 15.1) with a mean value of 66.25 ± 13.33 (SD) Bq kg^{-1} (Table 15.3), which are significantly lower than the prescribed value of 370 Bq kg^{-1} (UNSCEAR 2000).

15.3.2.2 Radiation Hazard Index (H_{ex})

External hazard index (H_{ex}) has commonly been employed (Agbalagba et al. 2012; Iqbal et al. 2000) to estimate the external exposure, which is defined as follows:

$$H_{\text{ex}} = \frac{A_{226\text{Ra}}}{370} + \frac{A_{232\text{Th}}}{259} + \frac{A_{40\text{K}}}{4810} \leq 1 \quad (15.5)$$

where, H_{ex} is a dimensionless quantity, since the unit of the denominator of Eq. (15.5) is also Bq kg^{-1} , (Farai and Ademola 2005). Corresponding to the upper allowable value of R_{eq} , the highest permissible value of H_{ex} can be ≤ 1 (Merdanoğlu and Altınoy 2006). Tables 15.1 and 15.2 provide the H_{ex} for the beach sand and soil samples of our study, varying from 0.100 to 0.231 with an average value of 0.179 ± 0.036 . All the calculated values of H_{ex} are less than 1, which implies that this island is radiologically safe for the local inhabitants as well for the tourists.

15.3.2.3 Absorbed Dose Rate (D)

The geographical characteristics govern the distribution of radiation exposure in a given place. Following UNSCEAR (2000) guideline, NORMs are supposed to be homogeneously distributed and the absorbed dose rates (D) owing to the terrestrial gamma radiations (from ^{226}Ra , ^{232}Th and ^{40}K) at 1 m above the ground level for public can be estimated using the following Eq. (15.6):

$$D(\eta\text{Gy h}^{-1}) = 0.462A_{226\text{Ra}} + 0.621A_{232\text{Th}} + 0.0417A_{40\text{K}} \quad (15.6)$$

where, 0.462, 0.621 and 0.0417 are the respective dose conversion factors transforming the radioactivities of NORMs into dose rates (in nGy h^{-1}). The D-value in air owing to the NORMs in the beach sand samples of our studied area range from 17.71 to 40.99 nGy h^{-1} with a mean value of 32.18 nGy h^{-1} (Table 15.2), which are significantly lower than the permissible value of 55 nGy h^{-1} for the public (Table 15.2) as prescribed in the UNSCEAR (2000). To pictorially represent the spatial distribution of cumulative contribution of NORMs, in Fig. 15.3d, absorbed dose rates are shown by IDW map.

15.3.2.4 Annual Effective Dose Rate (E_{ff})

Two aspects should be considered while calculating E_{ff} in outdoor (UNSCEAR 2000)-(a) the conversion factor from absorbed dose in air to the effective dose (0.7 Sv Gy^{-1}) and (b) the indoor occupancy factor (0.2). Therefore, the E_{ff} (in mSv y^{-1}) can be estimated by using the succeeding relation (15.7):

$$E_{\text{ff}}(\text{mSv y}^{-1}) = D(\eta\text{Gy h}^{-1}) \times 8760 \text{ h yr}^{-1} \times 0.7 \times \left(10^3 \frac{\text{mSv}}{10^9}\right) \eta\text{Gy}^{-1} \times 0.2 \quad (15.7)$$

Considering 8760 h as the total number of hours per year, the estimated E_{ff} from the beach sand samples vary from 0.022 to 0.050 mSv y^{-1} with an average value of

$0.040 \pm 0.008 \text{ mSv y}^{-1}$ which are significantly lower than the quoted world mean value of 0.07 mSv y^{-1} (Table 15.2).

15.3.2.5 Excess Lifetime Cancer Risk (ELCR)

The ELCR can be computed by the following Eq. (15.8) (ICRP 1990):

$$\text{ELCR} = E_{\text{ff}} \times \text{ALT} \times \text{RF} \quad (15.8)$$

where, average life time (ALT) is assumed to be 70 years and the risk factor (RF) is 5.0×10^{-5} for the public exposure (ICRP 1990). In this study, the computed values of ELCR for exposure to beach sand samples were found to be varied from 0.76×10^{-4} to 1.76×10^{-4} with an average value of $1.39 \times 10^{-4} \pm 0.27 \times 10^{-4}$ (Table 15.3), which are considerably lower than the average for world value 2.90×10^{-4} (Table 15.2). All the estimated radiological hazard indices are within the permissible limits. In terms of radiological safety, it can be concluded that the samples from St. Martin tourist area do not endanger human health and threat to the ambient environment.

15.3.3 Correlation Matrix Analysis

To identify the source of radionuclides and their relationship with the radiological hazard indices, the calculated correlation coefficients are appeared in Table 15.4. In the current work, a significant positive relationship was found among the measured radionuclides and risk indices which suggested that the emission of gamma radiation is from all radionuclides. While the determined radionuclides show a weak degree of association or insignificant correlation among them. It indicated that ^{226}Ra and ^{232}Th decay series exist in different mineral suites/rock types in the beach sand samples and differences in geochemical behaviors of these radionuclides were assumed.

Table 15.4 Mutual correlation matrix of radionuclides and sand properties of the St. Martin's Island, Bangladesh

	^{226}Ra	^{232}Th	^{40}K	Ra_{eq}	Dose
^{226}Ra	1				
^{232}Th	0.16	1			
^{40}K	0.259	0.223	1		
Ra_{eq}	0.596*	0.764**	0.688**	1	
Dose	0.593*	0.726**	0.735**	0.998**	1

* Correlation is significant at the 0.05 level (2-tailed)

** Correlation is significant at the 0.01 level (2-tailed)

15.4 Conclusion

This study reveals the distribution of ionizing radiation emitting NORMs (^{226}Ra , ^{232}Th and ^{40}K) in the beach sand and water of and around the only coral reefed island in the Bay of Bengal for the first time. Artificial radionuclides (^{134}Cs , ^{137}Cs) have not been detected in the present study. Activity concentrations of the radionuclides are almost homogeneously distributed across the island. The results of this study are assessed to check the compatibility of international and national values. Unlike the high background coastal areas of the world and the Bay of Bengal, activity concentrations of coastal areas of the St. Martin's island is significantly low and are within the limit of UNSCEAR (2000). Coral reefs of this island are assumed to obstacle the gathering of wave resistant heavy minerals (which are enriched with the NORMs). The estimated radiation hazard parameters including radium equivalent activity (Ra_{eq}), radiation hazard index (H_{ex}), absorbed dose rate (D), annual effective dose rate (E_{ff}) and excess lifetime cancer risk (ELCR) are lower than the admissible recommended limits. Results of this study will form reference data for the only coral reefed Island in the Bay of Bengal and will be considered as the baseline data for the future works.

Acknowledgements We are thankful to the technical personnel associated with this study, especially to the persons who helped us during sampling. Financial support from the Atomic Energy Research Establishments (AERE) of Bangladesh Atomic Energy Commission is also thankfully acknowledged.

Conflicts of Interest The authors declare that they have no conflict of interest.

Funding The authors express their gratitude to Research Center of Advanced Materials, King Khalid University, Saudi Arabia, for support (award number KKU/RCAMS/22).

References

- Agbalagba EO, Onoja RA (2011) Evaluation of natural radioactivity in soil, sediment and water samples in Niger Delta (Biseni) flood plain lakes, Nigeria. *J Environ Radioact* 102(7):667–671
- Agbalagba EO, Avwiri GO, Chad-Umoreh YE (2012) γ -Spectroscopy measurement of natural radioactivity and assessment of radiation hazard indices in soil samples from oil fields environment of Delta State, Nigeria. *J Environ Radioact* 109:64–70
- Ahmed MM, Das SK, Haydar MA, Bhuiyan MMH, Ali MI, Paul D (2014) Study of natural radioactivity and radiological hazard of sand, sediment, and soil samples from Inani Beach, Cox's Bazar, Bangladesh. *J Nucl Part Phys* 4(2):69–78
- Akhtar A (1992) Palynology of Girujan Clay, St. Martin's Island, Cox's Bazar District, Bangladesh. Geological survey of Bangladesh, Dhaka, vol 7(2), p 24
- Alam MN, Chowdhury MI, Kamal M, Ghose S, Isam MN, Mustafa MN, Miah MMH, Ansary MM (1999) The ^{226}Ra , ^{232}Th and ^{40}K activities in beach sand minerals and beach soils of Cox's Bazar, Bangladesh. *J Environ Radioact* 70:2652–2660
- Almayahi BA, Tajuddin AA, Jaafar MS (2012) Radiation hazard indices of soil and water samples in Northern Malaysian Peninsula. *Appl Radiat Isot* 57:109–119

- Asaduzzaman Kh, Mannan F, Khandaker MU, Farook MS, Elkezza A, Amin YM, Sharma S, Kassim HA (2015) Assessment of natural radioactivity levels and potential radiological risks of common building materials used in Bangladeshi dwellings. *PLoS ONE* 10(10):1–16
- Baltas H, Kiris E, Sirin M (2017) Determination of radioactivity levels and heavy metal concentrations in seawater, sediment and anchovy (*Engraulis encrasicolus*) from the Black Sea in Rize, Turkey. *Mar Pollut Bull* 116(1–2):528–533
- Begum M, Khan R, Hossain SM, Al Mamun SMMA (2022) Redistributions of NORMs in and around a gas-field (Shabazpur Bangladesh): radiological risks assessment. *J Radioanal Nucl Chem* 331(1):317–330. <https://doi.org/10.1007/s10967-021-08107-x>
- Farai IP, Ademola JA (2005) Radium equivalent activity concentrations in concrete building blocks in eight cities in Southwestern Nigeria. *J Environ Radioact* 79:119–125
- Freitas AC, Alencar AS (2004) Gamma dose rates and distribution of natural radionuclides in sand beaches—Ilha Grande, Southeastern Brazil. *J Environ Radioact* 75:211–223
- Ghosal S, Agrahari S, Guin R, Sengupta D (2017) Implications of modeled radioactivity measurements along coastal Odisha, Eastern India for heavy mineral resources. *Estuar Coast Shelf Sci* 184:83–89
- Habib MA, Khan R (2021) Environmental impacts of coal-mining and coal-fired power-plant activities in a developing country with global context. Spatial modeling and assessment of environmental contaminants (Chapter 24), environmental challenges and solutions, Springer Nature Switzerland AG. https://doi.org/10.1007/978-3-030-63422-3_24
- Habib MA, Khan R, Phoungthong K (2022) Evaluation of environmental radioactivity in soils around a coal burning power plant and a coal mining area in Barapukuria Bangladesh: radiological risks assessment. *Chem Geol* 600:120865. <https://doi.org/10.1016/j.chemgeo.2022.120865>
- Habib MA, Basuki T, Miyashita S, Bekelesi W, Nakashima S, Phoungthong K, Khan R, Rashid MB, Islam ARMT, Techato K (2018) Distribution of naturally occurring radionuclides in soil around a coal-based power plant and their potential radiological risk assessment. *Radiochim Acta* (accepted). <https://doi.org/10.1515/ract-2018-3044>
- Habib MA, Basuki T, Miyashita S, Bekelesi W, Nakashima S, Techato K, Khan R, Majlis ABK, Phoungthong K (2019) Assessment of natural radioactivity in coals and coal combustion residues from a coal-based thermoelectric plant in Bangladesh: implications for radiological health hazards. *Environ Monit Assess* (accepted). <https://doi.org/10.1007/s10661-018-7160-y>
- Huang Y, Lu X, Ding X, Feng T (2015) Natural radioactivity level in beach sand along the coast of Xiamen Island, China. *Mar Pollut Bull* 91:357–361
- ICRP (1990) Recommendations of the international commission on radiological protection. 21(1–3), publication 60
- Iqbal M, Tufail M, Mirza SM (2000) Measurement of natural radioactivity in marble found in Pakistan using a NaI (Tl) gamma-ray spectrometer. *J Environ Radioact* 51:255–265
- Islam AAMS, Khandaker MU, Miah MH, Hossain S (2019) Radioactivity in coral skeletons and marine sediments collected from the St. Martin’s Island of Bangladesh. *J Radioanal Nuclear Chem* (accepted). <https://doi.org/10.1007/s10967-019-06582-x>
- Jafarabadi AR, Bakhtiyari AR, Toosi AS, Jadot C (2017a) Spatial distribution, ecological and health risk assessment of heavy metals in marine surface sediments and coastal seawaters of fringing coral reefs of the Persian Gulf, Iran. *Chemosphere* 185:1090–1111
- Jafarabadi AR, Bakhtiyari AR, Aliabadian M, Toosi AS (2017b) Spatial distribution and composition of aliphatic hydrocarbons, polycyclic aromatic hydrocarbons and hopanes in superficial sediments of the coral reefs of the Persian Gulf, Iran. *Environ Pollut* 224:195–223
- Jafarabadi AR, Bakhtiyari AR, Maisano M, Pereira P, Cappello T (2018a) First record of bioaccumulation and bioconcentration of metals in Scleractinian corals and their algal symbionts from Kharg and Lark coral reefs (Persian Gulf, Iran). *Sci Total Environ* 640–641:1500–1511
- Jafarabadi AR, Bakhtiyari AR, Spanò N, Cappello T (2018b) First report of geochemical fractionation distribution, bioavailability and risk assessment of potentially toxic inorganic elements in sediments of coral reef Island of the Persian Gulf, Iran. *Mar Pollut Bull* 137:185–197

- Jafarabadi AR, Bakhtiari AR, Hedouin L, Toosi AS, Cappello T (2018c) Spatio-temporal variability, distribution and sources of *n*-alkanes and polycyclic aromatic hydrocarbons in reef surface sediments of Kharg and Lark coral reefs, Persian Gulf, Iran. *Ecotoxicol Environ Saf* 163:307–322
- Jafarabadi AR, Bakhtiari AR, Aliabadian M, Laetitia H, Toosi AS, Yap CK (2018d) First report of bioaccumulation and bioconcentration of aliphatic hydrocarbons (Ahs) and persistent organic pollutants (PAHs, PCBs and PCNs) and their effects on alcyonacea and scleractinian corals and their endosymbiotic algae from the Parsian Gulf, Iran: inter and intra-species differences. *Sci Total Environ* 627:141–157
- Joy A, Anoop PP, Rajesh R, Mathew J, Mathew A, Gopinath A (2019) Spatial variation of trace element concentration and contamination assessment in the coral reef sediments of Lakshdweep Archipelago, Indian Ocean. *Mar Pollut Bull* 146:106–116
- Kannan V, Rajan MP, Iyengar MAR, Ramesh R (2002) Distribution of natural and anthropogenic radionuclides in soil and beach sand samples of Kalpakkam (India) using hyper pure germanium (HPGe) gamma ray spectrometry. *Appl Radiat Isot* 57:109–119
- Khan FH (1964) Geology of St. Martin's Island: the geological survey of Pakistan records, vol X, pt 2-B, p 12
- Khan R, Islam HMT, Islam ARMT (2021) Mechanism of elevated radioactivity in Teesta river basin from Bangladesh: radiochemical characterization provenance and associated hazards. *Chemosphere* 264:128459. <https://doi.org/10.1016/j.chemosphere.2020.128459>
- Khan R, Rouf MA, Das S, Tamim U, Naher K, Podder J, Hossain SM, (2017) Spatial and multi-layered assessment of heavy metals in the sand of Cox's-Bazar beach of Bangladesh. *Reg Stud Mar Sci* 16:171–180. <https://doi.org/10.1016/j.rsma.2017.09.003>
- Khan R, Ghosal S, Sengupta D, Tamim U, Hossain SM, Agrahari S, (2018) Studies on heavy mineral placers from eastern coast of Odisha, India by instrumental neutron activation analysis. *J Radioanal Nucl Chem* (accepted). <https://doi.org/10.1007/s10967-018-6250-1>
- Khan R, Das S, Kabir S, Habib MA, Naher K, Islam MA, Tamim U, Rahman AKMR, Deb AK, Hossain SM (2019a) Evaluation of the elemental distribution in soil samples collected from ship-breaking areas and an adjacent island. *J Environ Chem Eng* (accepted). <https://doi.org/10.1016/j.jece.2019a.103189>
- Khan R, Islam HMT, Apon MAS, Islam ARMT, Habib MA, Phoungthong K, Idris AM, Techato K (2022) Environmental geochemistry of higher radioactivity in a transboundary Himalayan river sediment (Brahmaputra Bangladesh): potential radiation exposure and health risks. *Environ Sci Pollut Res*. <https://doi.org/10.1007/s11356-022-19735-5>
- Khan R, Parvez MS, Jolly YN, Haydar MA, Alam MF, Khatun MA, Sarker MMR, Habib MA, Tamim U, Das S, Sultana S, Islam MA, Naher K, Paul D, Akter S, Khan MHR, Nahid F, Huque R, Rajib M, Hossain SM (2019b) Elemental abundances, natural radioactivity and physicochemical records of a southern part of Bangladesh: implication for assessing the environmental geochemistry. *Environ Nanotechnol Monit Manag* (accepted). <https://doi.org/10.1016/j.enmm.2019b.100225>
- Khandaker MU, Jojo PJ, Kassim HA, Amin YM (2012) Radiometric analysis of construction materials using HPGe gamma-ray spectrometry. *Radiat Prot Dosim* 152:33–37
- Khandaker MU, Mohd Nasir NL, Asaduzzaman K, Olatunji MA, Amin YM, Kassim HA, Alrefae T (2016) Evaluation of radionuclides transfer from soil-to-edibleflora and estimation of radiological dose to the Malaysian populace. *Chemosphere* 154:528–536
- Khandaker MU, Mohd Nasir NL, Zakirin NS, Kassim HA, Asaduzzaman K, Bradley DA, Zulkifly MY, Hayyan A (2017) Radiation dose to the Malaysian populace via the consumption of bottled mineral water. *Radiat Phys Chem* 140:173–179
- Khandaker MU, Asaduzzaman K, Sulaiman AFB, Bradley DA, Isinkaye MO (2018) Elevated concentrations of naturally occurring radionuclides in heavy mineral-rich beach sands of Langkawi Island, Malaysia. *Mar Pollut Bull* 127:654–663
- Kucukomeroglu B, Karadeniz A, Damla N, Yesilkanat CM, Cevik U (2016) Radiological maps in beach sands along some coastal region of Turkey. *Mar Pollut Bull* 112:255–264

- Lewis SE, Lough JM, Cantin NE, Matson EG, Kinsley L, Bainbridge ZT, Brodie JE (2018) A critical evaluation of coral Ba/Ca, Mn/Ca and Y/Ca ratios as indicators of terrestrial input: New data from the Great Barrier Reef, Australia. *Geochim Cosmochim Acta* 237:131–154
- Lin W, Yu K, Wang Y, Liu X, Ning Q, Huang X (2019) Radioactive level of coral reefs in the South China Sea. *Mar Pollut Bull* 142:43–53. <https://doi.org/10.1016/j.marpolbul.2019.03.030>
- Mahawatte P, Fernando KNR (2013) Radioactivity levels in beach sand from the West Coast of Sri Lanka. *J Natn Sci Found Sri Lanka* 41(4):279–285
- Majlis ABK, Habib MA, Khan R, Phoungthong K, Techato K, Islam MA, Nakashima S, Islam ARMT, Hood MA, Hower JC (2022) Intrinsic characteristics of coal combustion residues and their environmental impacts: a case study for Bangladesh. *Fuel* 324:124711. <https://doi.org/10.1016/j.fuel.2022.124711>
- Margineanu RM, Dului OG, Blebea-Apostu AM, Gomoiu C, Bercea S (2013) Environmental dose-rate distribution along the Romanian Black Sea shore. *J Radioanal Nucl Chem* 298:1191–1196
- Merdanoğlu B, Altınsoy N (2006) Radioactivity concentrations and dose assessment for soil samples from Kestanbol granite area, Turkey. *Radiatprot Dosim* 121(4):399–405
- Mohanty AK, Sengupta D, Das SK, Saha SK, Van KV (2004) Natural radioactivity and radiation exposure in the high background area at Chhatrapur beach placer deposit of Orissa, India. *J Environ Radioact* 75:15–33
- Mokhtar MB, Praveena SM, Aris AZ, Yong OC, Lim AP (2012) Trace metal (Cd, Cu, Fe, Mn, Ni and Zn) accumulation in Scleractinian corals: a record for Sabah, Borneo. *Mar Pollut Bull* 64:2556–2563
- Papadopoulos A, Koroneos A, Christofides G, Papadopoulou L, Tzifas I (2016) Assessment of gamma radiation exposure of beach sands in highly touristic areas associated with plutonic rocks of the Atticocycladic zone (Greece). *J Environ Radioact* 162–163:235–243
- Prouty NG, Field ME, Stock JD, Jupiter SD, McCulloch M (2010) Coral Ba/Ca records of sediment input to the fringing reef of the southshore of Molokā'i, Hawai'i over the last several decades. *Mar Pollut Bull* 60:1822–1835
- Prouty NG, Goodkin NF, Jones R, Lamborg CH, Storlazzi CD, Hughen KA (2013) Environmental assessment of metal exposure of corals living in Castle Harbour, Bermuda. *Mar Chem* 154:55–66
- Rao NS, Sengupta D, Guin R, Saha SK (2009) Natural radioactivity measurements in beach sand along southern coast of Orissa, eastern India. *Environ Earth Sci* 59:593–601
- Rudnick RL, Gao S (2014) Composition of the continental crust. *Treatise on geochemistry*, 2nd edn, Chapter 4, pp 1–64
- Saha N, Webb GE, Zhao J (2016) Coral skeletal geochemistry as a monitor of inshore water quality. *Sci Total Environ* 566–567:652–684
- Saha N, Rodriguez-Ramirez A, Nguyen AD, Clark TR, Zhao J, Webb GE (2018) Seasonal to decadal scale influence of environmental drivers on Ba/Ca and Y/Ca in coral aragonite from the southern Great Barrier Reef. *Sci Total Environ* 639:1099–1109
- Saha N, Webb GE, Zhao J, Nguyen AD, Lewis SE, Lough JM (2019) Coral-based high resolution rare earth element proxy for terrestrial sediment discharge affecting coastal seawater quality, Great Barrier Reef. *Geochim Cosmochim Acta* 254:173–191
- Shuaibu HK, Khandaker MU, Alrefae T, Bradley DA (2017) Assessment of natural radioactivity and gamma-ray dose in monazite rich black sand beach of Penang Island, Malaysia. *Mar Pollut Bull* 119(1):423–428
- Tomascik T (1997) Management plan for coral resources of Narikel Jinjira (St. Martin's Island). Final Report, National Conservation Strategy Implementation Project-1, Ministry of Environment and Forest, Government of Bangladesh, p 125
- Tufail M (2012) Radium equivalent activity in the light of UNSCEAR report. *Environ Monit Assess* 184:5663–5667

- UNSCEAR (2000) Sources and effects of ionizing radiation; United Nations; Report to the General Assembly, with Scientific Annexes. United Nations (A/55/46), New York
- Zare MR, Kamali M, Omid Z, Khorambagheri M, Mortazavi MS, Ebrahimi M, Akbarzadeh G (2015) Evaluation of natural radioactivity content in high-volume surface water samples along the northern coast of Oman Sea using portable high-resolution gamma-ray spectrometry. *J Environ Radioact* 144:134–139